

EMISSION, ABSORPTION AND PROPAGATION OF ACOUSTIC THz-WAVES IN SOLIDS*

W. EISENMENGER

Physikalisches Institut der Universität Stuttgart, Teilinstitut 1
(Pfaffenwaldring 57, 7000 Stuttgart 80, FRG)

Recent experimental developments in generation and detection of THz acoustical phonons have led to studies of phonon emission, propagation and absorption in solids. New results of this acoustical phonon spectroscopy concern phonon interactions with collective excitations (phonons, photons, magnons), localized excitations (resonant scattering of impurities, radiationless transitions) and electronic excitations in metals, superconductors and semiconductors. The different experimental methods and their applications to phonon interaction studies are discussed.

Introduction

During the past ten years several new methods have been developed extending the classical range of ultrasound and microwave acoustics in solids into the range of THz (10^{12} Hz) and higher frequencies. The reason for this was an increasing interest in energy transport properties in solids in the range of thermal lattice vibration frequencies. Typical questions are: the mechanisms of heat generation or the emission of phonons by excited electrons and the resonance absorption and emission of mechanical vibrations or phonons by impurities in dielectric crystals. In analogy to optical spectroscopy this kind of investigation is called *phonon spectroscopy* in the sense of an acoustical emission and absorption spectroscopy. Since phonons and photons as Bose-particles are subject to the same quantum statistics, the well-known close analogy of waves between acoustics and microwave technique extends also into the range of THz frequencies. But also the quantum laws of radiation transitions, as for instance

* FASE-78, invited paper, unpublished in the Proceedings.

valid for atomic emission, photoeffect or bremsstrahlung are as valid for phonons as for photons. In consequence of the short wavelength of 10 \AA to 100 \AA a coherent detection in ultrasonics and microwave acoustics is not possible any more.

In the following we report on the progress in spectroscopy with acoustical phonons in the THz-frequency range. We discuss different experimental methods and the phonon interactions which have been investigated.

Inelastic neutron scattering

From the Bragg scattering of monochromatic thermal neutrons by thermal sound waves or sound waves due to quantum mechanical zero-point oscillations the total $\omega(k)$ -relation or dispersion curve of the possible lattice vibrations of the crystal is obtained, as shown in Fig. 1. By the presently available high neutron densities in high flux reactors a frequency resolution of 50 GHz

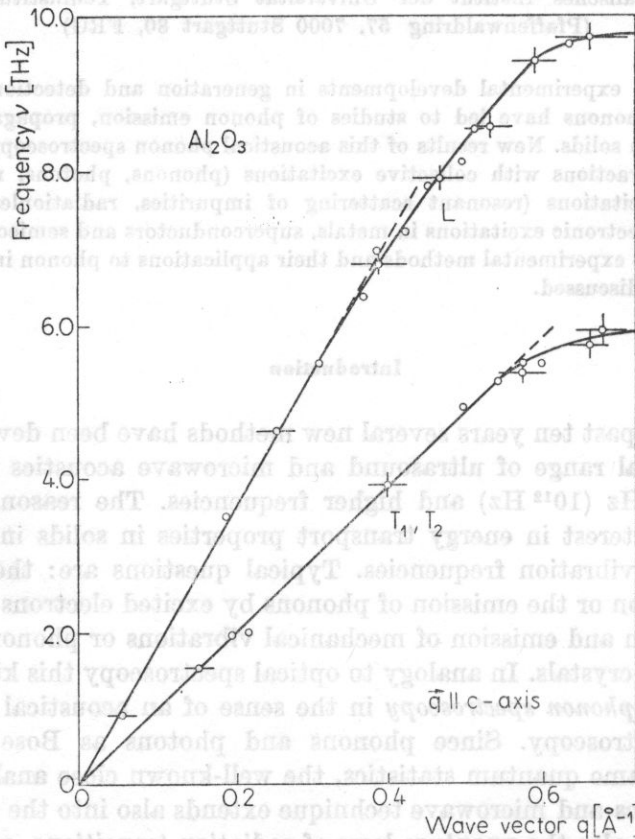


Fig. 1. Dispersion of acoustical phonons in Al_2O_3 obtained from neutron scattering (H. Bialas et al., Phys. Lett. 43, 97, 1973)

is attainable. In consequence of this high resolution it is meanwhile possible, as shown in Fig. 2, to detect the influence of localized lattice vibrations [1] on the dispersion curve resulting from high concentrations of impurity atoms. Under the influence of localized oscillations the dispersion curve splits at the frequency of the impurity resonance. While the method of neutron scattering is superior to any other method for the determination of the acoustic dispersion,

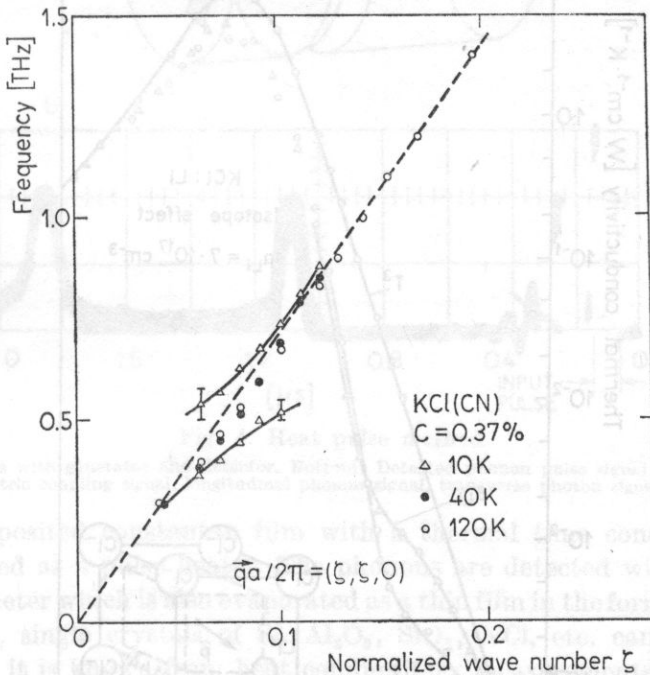


Fig. 2. Splitting of the acoustical phonon dispersion by the localized impurity resonance in KCl CN ([1], R. M. Nicklow)

i.e. the phonon $\omega(k)$ relation of the crystal, it is not well suited for the determination of acoustic attenuation or of the mean free path of phonons propagating in the solid. This is especially valid for the resonance scattering by impurities of lower concentration. Also the analysis of phonon emission spectra is very difficult in consequence of the low sensitivity.

Thermal conductivity and phonon pulse measurements

One of the best known and simplest methods to determine the scattering of THz phonons in solids is the measurement of heat conduction, especially in the range of low temperatures. Beside the influence of sample geometry and elastic scattering, especially Rayleigh-scattering, on the phonon mean free

path, information on inelastic phonon scattering (Umklapp-processes) and electron scattering can be obtained. In addition, minima in the heat conductivity as function of temperature show the influence of resonant phonon scattering by impurities as e.g. paraelectric systems [2], i.e., KCl:Li (as shown in Fig. 3), paramagnetic ions and ions with splitting of the electronic energy

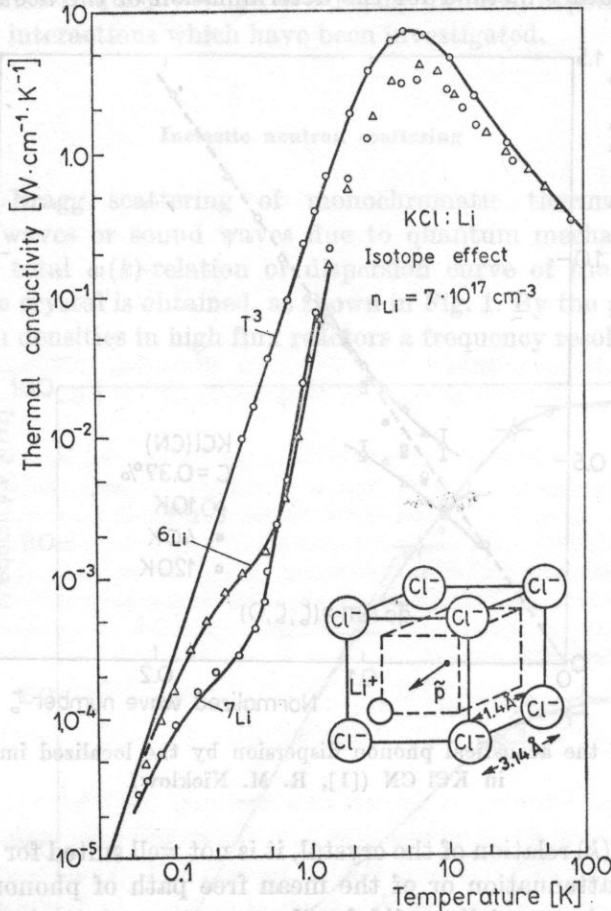


Fig. 3. Tunneling resonance of Li in KCl observed in thermal conductivity [2]

states by crystal field effects [3] (i.e. $\text{Al}_2\text{O}_3 : \text{V}^{3+}$, $\text{Al}_2\text{O}_3 : \text{Ti}^{3+}$). The frequency resolution of these measurements is very poor, also the mode dependence of the phonon scattering cannot be determined.

A significant progress was possible by the introduction of the heat pulse method [4] by v. GUTFELD and NETHERCOT. In this method (see Fig. 4) a separate measurement of the propagation of longitudinal and transverse phonon pulses is possible. In addition, the contribution of diffusely scattered phonons can be determined. For the generation of phonon pulses in heat pulse experiments

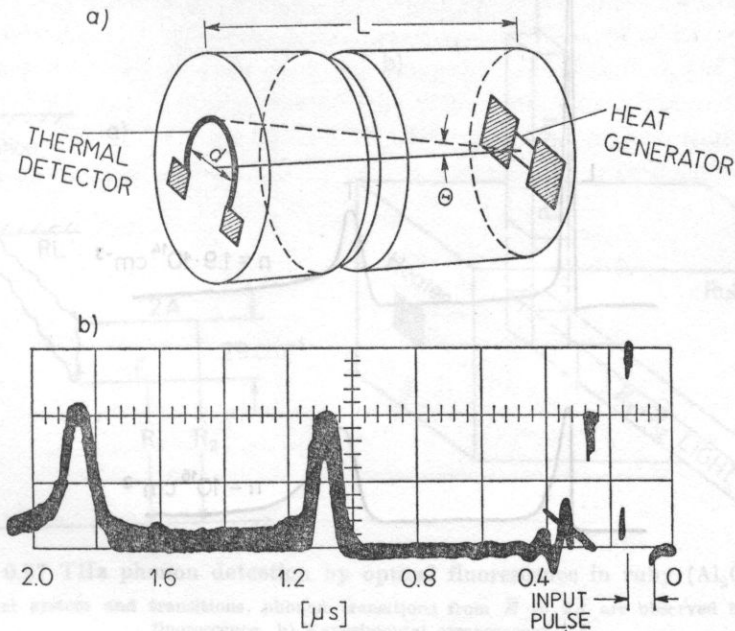


Fig. 4. Heat pulse method

Top: crystal sample with generator and detector. Bottom: Detected phonon pulse signal. From right to left, electric coupling signal, longitudinal phonon signal, transverse phonon signal [4]

a vacuum deposited constantan film with a thermal time constant of about 10^{-8} sec is used as a pulse heater. The phonons are detected with a superconducting bolometer which is also evaporated as a thin film in the form of a meander. As substrates, single crystals of Si, Al_2O_3 , SiO_2 , KCl, etc. can be used. For these crystals it is known from heat conductivity measurements that the phonon mean free path exceeds the order of 1 cm which corresponds to the mostly used sample dimensions. The measuring temperature is determined by the superconducting transition temperature of the bolometer (Al: 1.2 K; Sn: 3.7 K). The differences in the propagation of longitudinal and transverse phonons have been demonstrated very clearly in a phonon propagation experiment [5] in undoped and degenerately doped n -InSb (see Fig. 5). While longitudinal and transverse phonons propagate almost undamped in undoped InSb (mean free path 1 cm), the longitudinal wave is strongly attenuated in degenerate n -doped InSb by inelastic electron scattering at the spherical Fermi surface. Heat pulse measurements have been very valuable in investigations of phonon propagation velocities and of phonon focussing [6] by anisotropy of the sound velocity as well as in phonon scattering measurements. Since phonon generation by heaters and detection by bolometers are experimentally uncomplicated, these techniques are often used in connection with other detection or phonon generation methods. The high maximum phonon radiation power of the generator and the great sensitivity of the detector, as well as the fact that

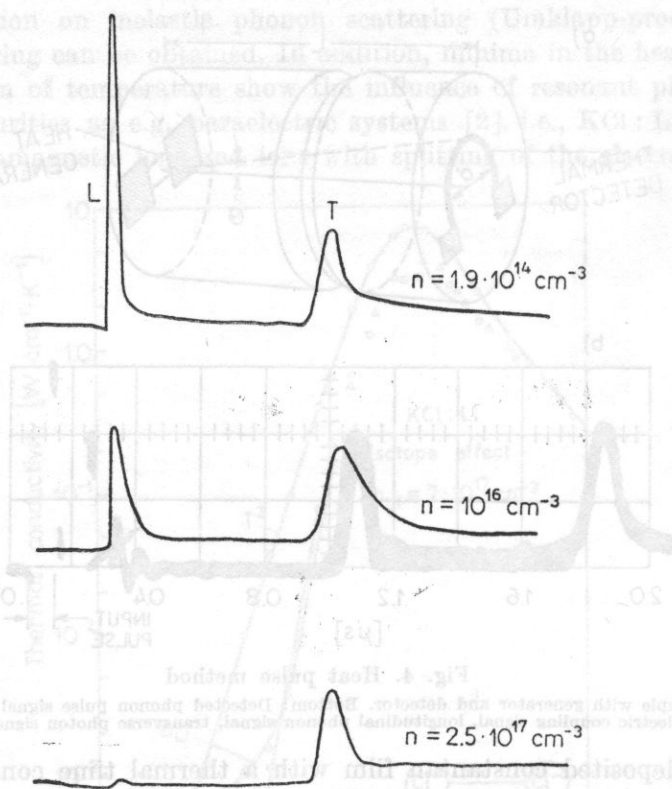


Fig. 5. Attenuation of longitudinal heat pulses in the degenerately doped n -InSb with increasing carrier concentration [5]

thin metal layers can be evaporated on arbitrary crystal surfaces which have been polished, are of great advantage.

To a certain extent, frequency information, however, with poor resolution can be obtained as in heat conduction measurements by variation of the heater power or the heater temperature.

Frequency selective phonon detection by induced optical fluorescence of crystal ions

The first successful frequency selective phonon detection in the THz range by influencing the optical fluorescence was reported by RENK and DEISENHOFER [7] who used the system $\text{Al}_2\text{O}_3 : \text{Cr}^{3+}$. In this experiment (see Fig. 6) the splitting of the metastable ruby laser levels in the so-called \bar{E} and $2\bar{A}$ -states with a spacing of 29 cm^{-1} , corresponding to 0.87 THz , is used. Using ultraviolet excitation of the crystal at low temperatures the optical fluorescence is mainly observed from the lower \bar{E} -level. The $2\bar{A}$ -level is weakly populated in consequence of fast radiationless transitions to the \bar{E} -level. Phonon radiation

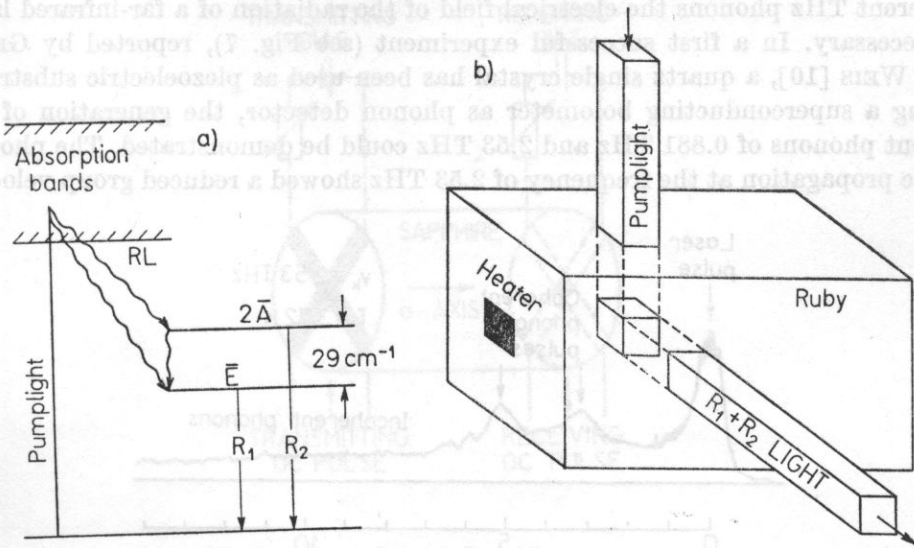


Fig. 6. 0.87 THz phonon detection by optical fluorescence in ruby ($\text{Al}_2\text{O}_3 : \text{Cr}^{3+}$)

a) Energy level system and transitions, phonon transitions from \bar{E} to $2\bar{A}$ are observed by enhanced R_2 fluorescence. b) Experimental arrangement [7]

at 0.87 THz increases the population of the $2\bar{A}$ -level by additional transitions from the \bar{E} -level under phonon absorption. Correspondingly, the phonon population at the frequency of 0.87 THz can be determined by observing the R_2 -fluorescence intensity. Heat pulse experiments demonstrated the possibility of a fast and sensitive phonon detection. In addition, phonon trapping and the coupling of metastable states in the phonon field could be investigated. Recent experiments have also been performed with the system $\text{CaF}_2 : \text{Eu}^{2+}$. This system shows a pressure-dependent level splitting [8] of radiationless transitions in the frequency range from 0 to 80 cm^{-1} corresponding to the frequency range from 0 to 2.4 THz. In principle, systems of this kind are well suited for monochromatic phonon detection and also for generating incoherent phonons. A further possibility of optical phonon detection and phonon generation lies in the application of vibronic side lines of fluorescence transitions [9] of rare earth ions. In this respect the system $\text{SrF}_2 : \text{Eu}^{2+}$ has been used for an analysis of the phonon spectrum radiated from a pulse heater. These optical methods have so far been applied to special systems, an extension to other substrates appears possible if special coupling methods or surface doping are used.

Coherent surface excitation of THz phonons

The methods discussed so far concerned the detection and generation of incoherent phonons. In contrast, coherent phonons can be generated by surface excitation of piezoelectric crystals in the field of microwaves. For generating

coherent THz phonons the electrical field of the radiation of a far-infrared laser is necessary. In a first successful experiment (see Fig. 7), reported by GRILL and WEIS [10], a quartz single crystal has been used as piezoelectric substrate. Using a superconducting bolometer as phonon detector, the generation of coherent phonons of 0.881 THz and 2.53 THz could be demonstrated. The phonon pulse propagation at the frequency of 2.53 THz showed a reduced group velocity

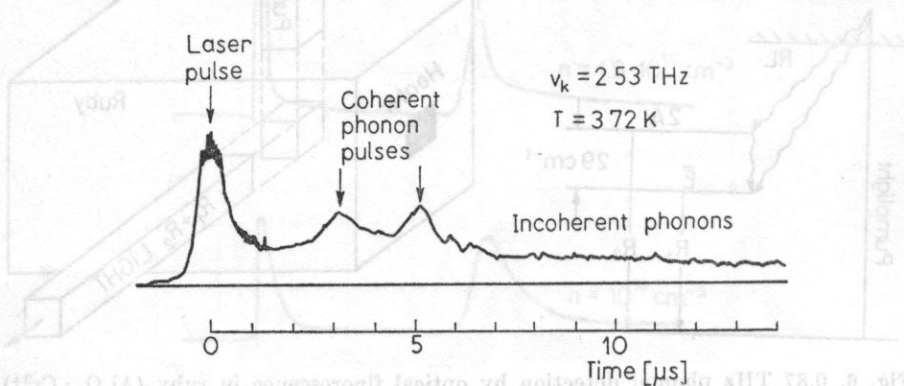


Fig. 8. 0.87 THz phonon generation by optical fluorescence in ruby ($\text{Al}_2\text{O}_3:\text{Cr}^{3+}$). (a) Energy level system and transition phonon transitions from \bar{K} to \bar{K} as observed by enhanced fluorescence. (b) Experimental arrangement.

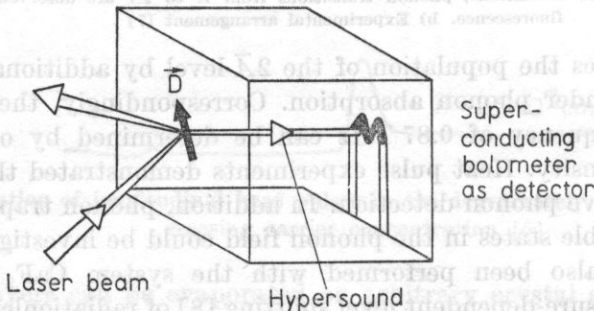


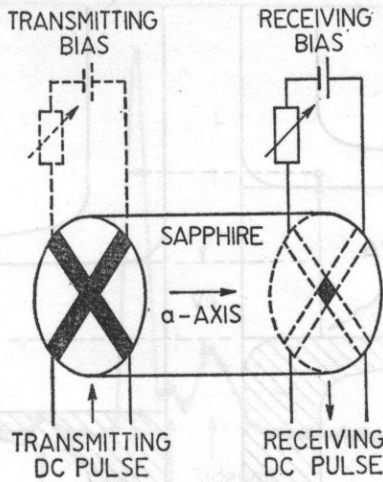
Fig. 7. Coherent THz phonon generation by FIR surface excitation of quartz

Top: phonon pulses by bolometer detection. Bottom: experimental arrangement [10]

compared to the propagation of phonons with lower frequencies in agreement with the dispersion in crystalline quartz. Coherent phonons in the THz frequency range can be used for the investigation of saturation and other high intensity effects. A spectroscopy with coherent acoustical phonons necessitates continuously tunable far-infrared laser sources.

Phonon spectroscopy with superconducting tunneling junctions

For a versatile spectroscopy with acoustic phonons in the THz range it is necessary for the phonon generator and detector to be easily deposited on the substrate surface (see Fig. 8) (as e.g. by vacuum evaporation) and that, in ad-



TRANSMITTING PULSE RANGE

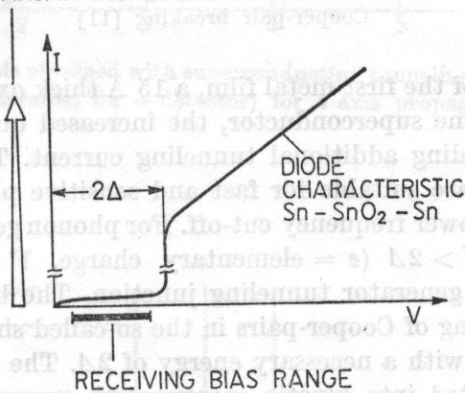


Fig. 8. Phonon generation and detection with superconducting tunneling junctions. Top: experimental arrangement. Bottom: Tunneling I - V characteristic with detection and transmitting bias range [11]

dition, generator or detector can be tuned. These conditions are fulfilled to a wide extent for superconducting tunneling junctions [11]. Phonon detection (see Fig. 9) is analogous to the internal photoelectric effect. Phonons having a minimum energy of 2Δ (Δ = energy gap) excite electrons from the superconducting ground state by breaking-off Cooper-pairs. The mean free phonon path for this process is of the order of 1000 \AA at frequencies corresponding to $h\nu = 2\Delta$ ($2\Delta_{\text{Al}} = 0.38 \text{ meV}$ or 90 GHz , $2\Delta_{\text{Sn}} = 1.2 \text{ meV}$ or 290 GHz ; $2\Delta_{\text{Pb}} = 2.7 \text{ meV}$ or 650 GHz). In a vacuum deposited superconducting film of appr. 2000 \AA thickness phonons of the energy exceeding 2Δ are, therefore, nearly completely absorbed leading to an increase of the electron or quasiparticle density exceeding the thermal occupation. In a superconducting tunneling

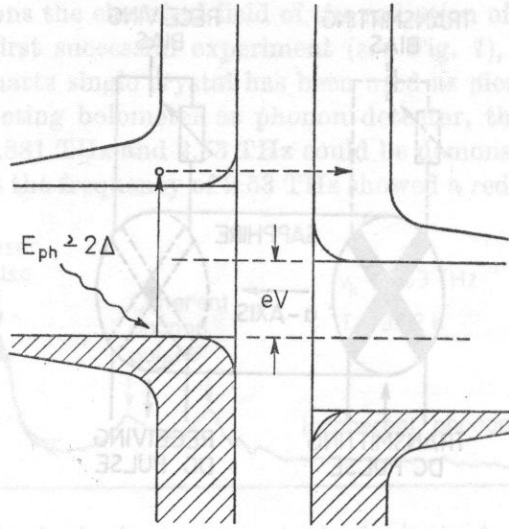


Fig. 9. Phonon detection ($0 < eV < 2\Delta$) with superconducting tunneling junctions by Cooper-pair breaking [11]

junction, consisting of the first metal film, a 15 \AA thick oxide layer and a second metal film of the same superconductor, the increased quasiparticle population leads to a corresponding additional tunneling current. Thus, superconducting tunneling junctions are suitable for fast and sensitive phonon pulse detection (see Fig. 10) with a lower frequency cut-off. For phonon generation a DC-voltage corresponding to $eV > 2\Delta$ ($e =$ elementary charge, $V =$ battery voltage) is applied to a similar generator tunneling junction. The battery voltage is sufficient for the breaking of Cooper-pairs in the so-called single particle tunneling process (see Fig. 11) with a necessary energy of 2Δ . The excess energy $eV - 2\Delta$ is essentially converted into kinetic energy of the quasiparticles. This excess energy can be emitted by quasiparticle relaxation to the gap edge Δ in the form of relaxation phonons. This process is analogous to the X-ray bremsstrahlung. After the relaxation decay the quasiparticles recombine again to Cooper-pairs emitting phonons of the fixed frequency corresponding to $h\nu = 2\Delta$. The energy distribution of the relaxation phonons exhibits a sharp upper limit at $eV - 2\Delta$. The special form of the quasiparticle density of states in the superconductor leads to a nearly rectangular spectral distribution at this cut-off frequency. For the spectroscopy [12] with phonons (see Fig. 12) it is now essential that using a modulation of the generator voltage $V \pm \delta V$ leads only to a spectral change at the frequency $\nu = (eV - 2\Delta) : h$ in a narrow band of the width $\delta\nu = \pm \delta eV : h$. The resulting modulation of the detector signal, therefore, contains only the signal contributions from this narrow frequency band which is tunable by varying the generator voltage. In this way a spectroscopy with quasimonochromatic phonons is possible which meanwhile has found several

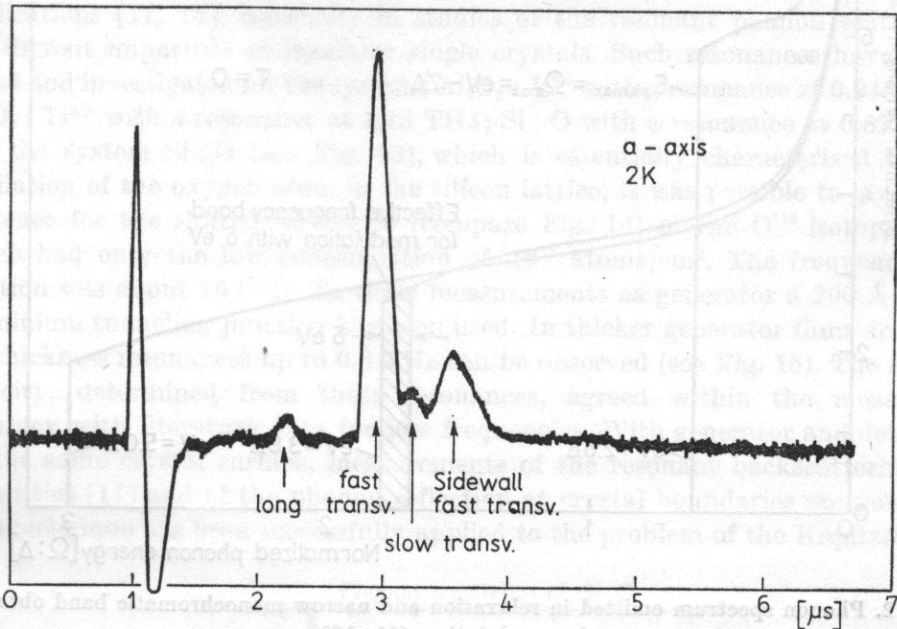


Fig. 10. Phonon pulse signals obtained with superconducting tunneling junctions as generator and detector (Pb - generator, Sn - detector) for a -axis propagation in Al_2O_3 [11]

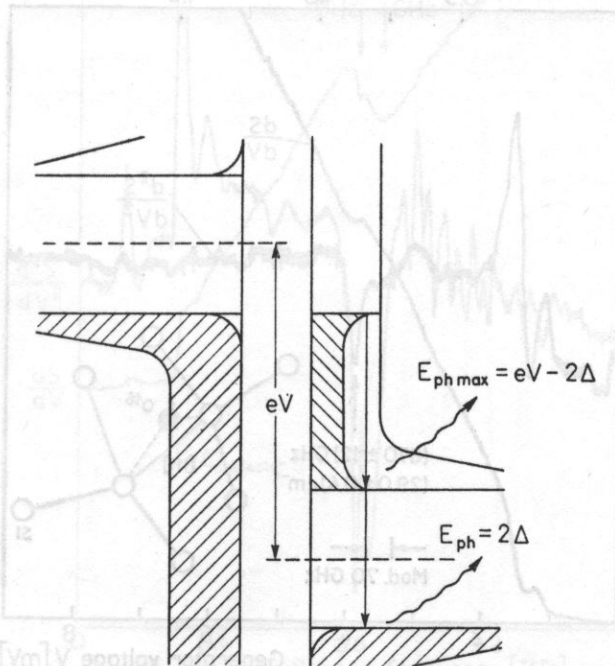


Fig. 11. Phonon frequency ($eV > 2\Delta$) in superconducting tunneling junctions
 Relaxation: $E_{ph\max} = eV - 2\Delta$. Recombination: $E_{ph} = 2\Delta$ [11]

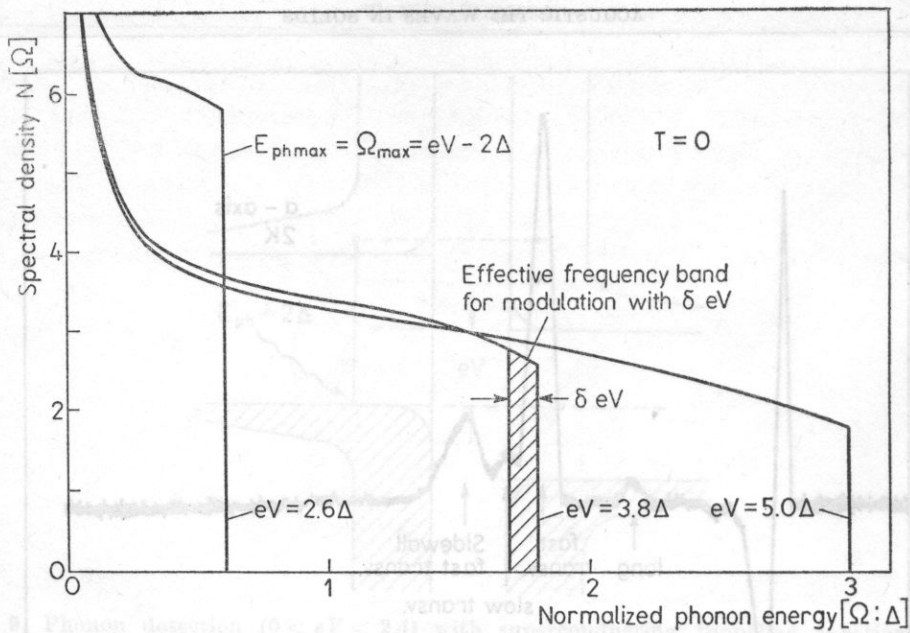


Fig. 12. Phonon spectrum emitted in relaxation and narrow monochromatic band obtained by modulation [11, 12]

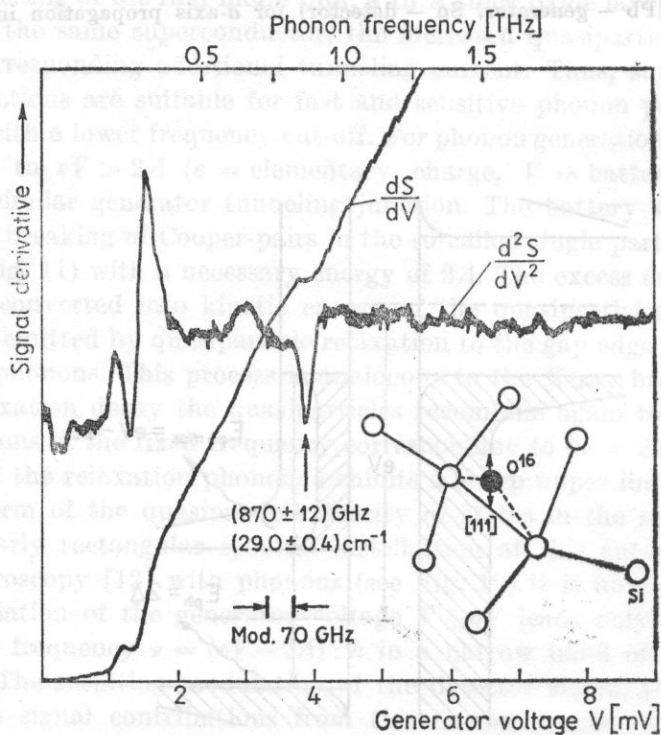


Fig. 13. 870 GHz phonon absorption by oxygen in Si

dS/dV = first detector-generator derivative or direct modulation signal; d^2S/dV^2 = second detector - generator derivative or second harmonic modulation signal

applications [11, 14], especially in studies of the resonant phonon scattering of different impurities in insulator single crystals. Such resonances have been found and investigated for the systems $\text{Al}_2\text{O}_3 : \text{V}^{3+}$ with a resonance at 0.248 THz; $\text{Al}_2\text{O}_3 : \text{Ti}^{3+}$ with a resonance at 1.13 THz; $\text{Si} : \text{O}$ with a resonance at 0.87 THz. For the system $\text{Si} : \text{O}$ (see Fig. 13), which is essentially characterized by an oscillation of the oxygen atom in the silicon lattice, it was possible to give also evidence for the shifted resonance (compare Fig. 14) of the ^{18}O isotope [13] which had only the low concentration of 10^{18} atoms/cm³. The frequency resolution was about 10 GHz. In these measurements as generator a 200 Å thick aluminium tunneling junction has been used. In thicker generator films acoustical thickness resonances up to 0.8 THz can be observed (see Fig. 15). The sound velocity, determined from these resonances, agreed within the measuring accuracy with literature data for low frequencies. With generator and detector on the same crystal surface, measurements of the resonant backscattering by impurities [14] and of the phonon reflection at crystal boundaries are possible. This technique has been successfully applied to the problem of the Kapitza-an-

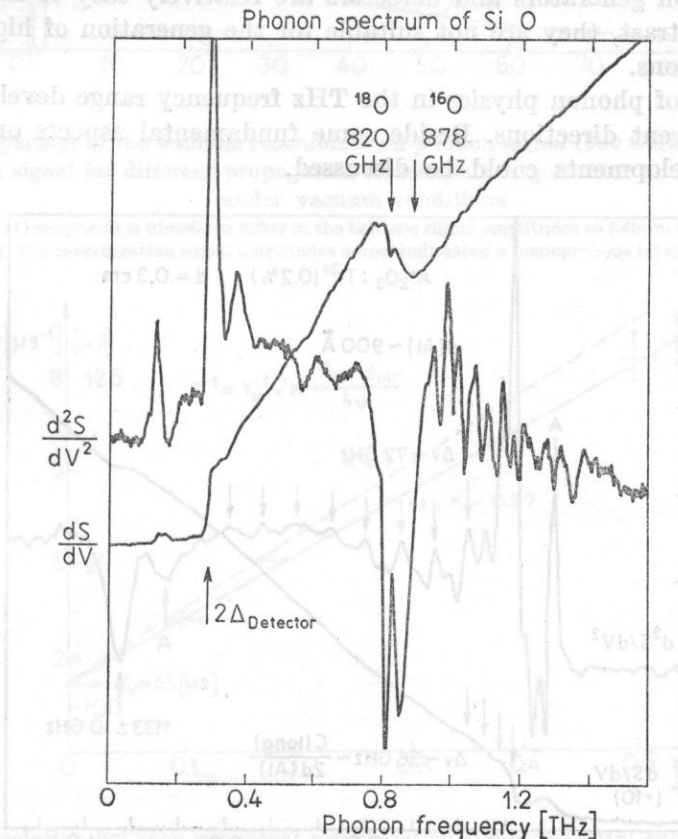


Fig. 14. ^{18}O isotope phonon resonance absorption

In the range 0.9 to 1.3 THz additional resonance structure indicates new vibrational processes [13]

maly, i.e. the transmission of phonons from the crystal into liquid helium [15]. In addition, the phonon emission spectrum [16, 13] of superconducting tunneling junctions could be investigated in detail confirming the predictions of the theory of superconductivity. Measurements of the phonon intensities emitted by recombination of quasiparticles to Cooper-pairs indicated that even for ideal crystals and crystal surfaces the total absorption of phonons amounts to about 90%. Terahertz phonon reverberation measurements [17] in the crystal substrate analogous to the room acoustical reverberation method (see Figs. 16 and 17) showed that the responsible phonon absorption processes are not localized in the crystal volume, but at the interface between the superconducting tunneling junction and the crystal substrate. In this process THz phonons decay in a wide frequency range spontaneously into low energy acoustical phonons. Other investigations concerned insulators, semiconductors, metals and superconductors, by which new results with respect to the phonon interaction with impurities, magnons and electrons have been obtained.

Beside their tunability discussed above, superconducting tunneling junctions as phonon generators and detectors are relatively easy to fabricate and to use. In contrast, they are not suitable for the generation of high intensity coherent phonons.

The field of phonon physics in the THz frequency range develops already in many different directions. Beside some fundamental aspects only some of the main developments could be discussed.

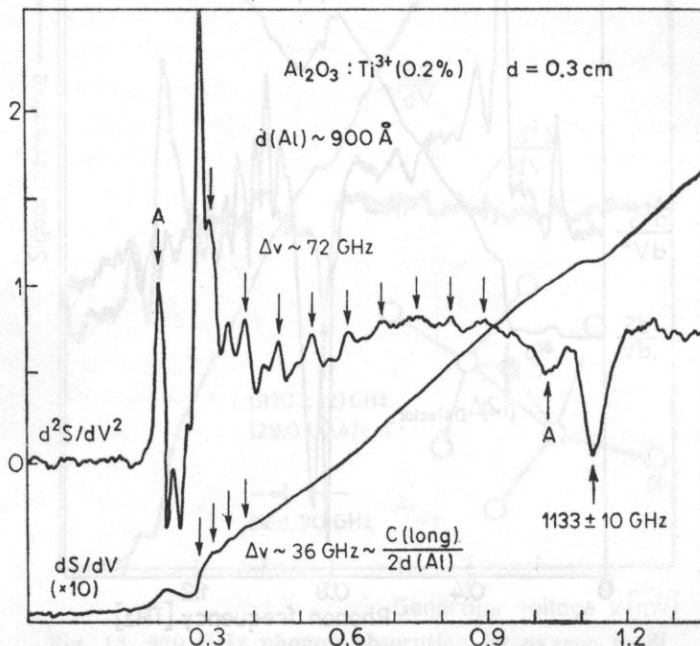


Fig. 15. Acoustical phonon absorption in $\text{Al}_2\text{O}_3 : \text{Ti}^{3+}$ at 1.13 THz (A = precursor, reduced at lower temperature), $\Delta\nu = 72$ GHz

Generator film thickness resonance modes indicate sound velocity in agreement with bulk values

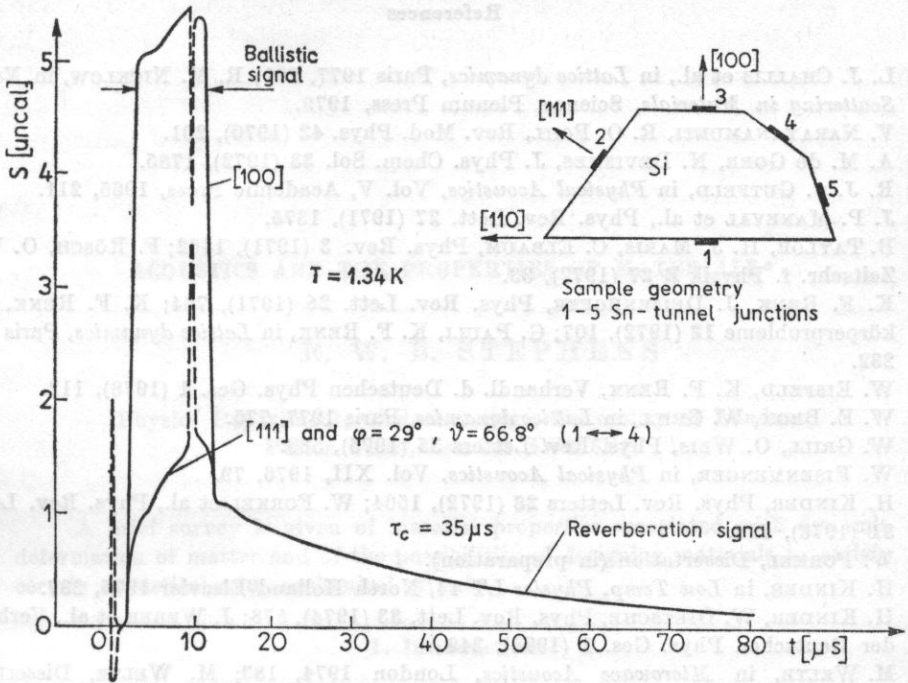


Fig. 16. Comparison of the ballistic recombination phonon signal (280 GHz) and the phonon reverberation signal for different propagation directions and generator or detector positions under vacuum conditions

The (100) and (111) propagation directions differ in the ballistic signal amplitudes as follows from different phonon focussing factors. The reverberation signal amplitudes agree, indicating a homogeneous intensity distribution [17]

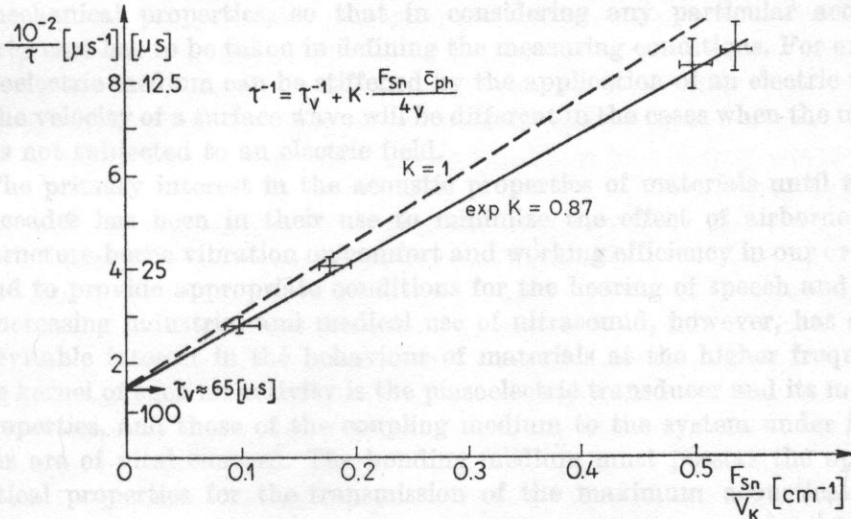


Fig. 17. The relation between reciprocal reverberation time (280 GHz) and the ratio of the Sn-covered surface area to the Si-crystal volume. The resulting experimental absorption constant $K = 0.87$ is in agreement with the ballistic experiments. Further analysis indicates the importance of interface loss processes [17]

References

- [1] L. J. CHALLIS et al., in *Lattice dynamics*, Paris 1977, 261; R. M. NICKLOW, in *Neutron Scattering in Materials*, Science, Plenum Press, 1979.
- [2] V. NARAYANAMURTI, R. O. POHL, *Rev. Mod. Phys.* **42** (1970), 201.
- [3] A. M. de GOER, N. DEVISMES, *J. Phys. Chem. Sol.* **33** (1972), 1785.
- [4] R. J. v. GUTFELD, in *Physical Acoustics*, Vol. V, Academic Press, 1965, 211.
- [5] J. P. MANEVAL et al., *Phys. Rev. Lett.* **27** (1971), 1375.
- [6] B. TAYLOR, H. J. MARIS, C. ELBAUM, *Phys. Rev.* **3** (1971), 1462; F. RÖSCH, O. WEIS, *Zeitschr. f. Physik B* **27** (1977), 33.
- [7] K. F. RENK, J. DEISENHOFER, *Phys. Rev. Lett.* **26** (1971), 764; K. F. RENK, *Festkörperprobleme* **12** (1972), 107; G. PAULI, K. F. RENK, in *Lattice dynamics*, Paris 1977, 232.
- [8] W. EISFELD, K. F. RENK, *Verhandl. d. Deutschen Phys. Ges.* **1** (1978), 112.
- [9] W. E. BRON, W. GRILL, in *Lattice dynamics*, Paris 1977, 775.
- [10] W. GRILL, O. WEIS, *Phys. Rev. Letters* **35** (1975), 588.
- [11] W. EISENMENGER, in *Physical Acoustics*, Vol. XII, 1976, 79.
- [12] H. KINDER, *Phys. Rev. Letters* **28** (1972), 1564; W. FORKEL et al., *Phys. Rev. Letters* **31** (1973), 215.
- [13] W. FORKEL, Dissertation (in preparation).
- [14] H. KINDER, in *Low Temp. Physics* LT 14, North Holland/Elsevier 1975, 287.
- [15] H. KINDER, W. DIETSCH, *Phys. Rev. Lett.* **33** (1974), 578; J. WEBER et al., *Verhandl. der Deutschen Phys. Ges.* **1** (1978), 349.
- [16] M. WELTE, in *Microwave Acoustics*, London 1974, 183; M. WELTE, Dissertation (in preparation).
- [17] H. J. TRUMPP, W. EISENMENGER, *Z. Physik, B* **23** (1977), 159.

Received on February 16, 1978

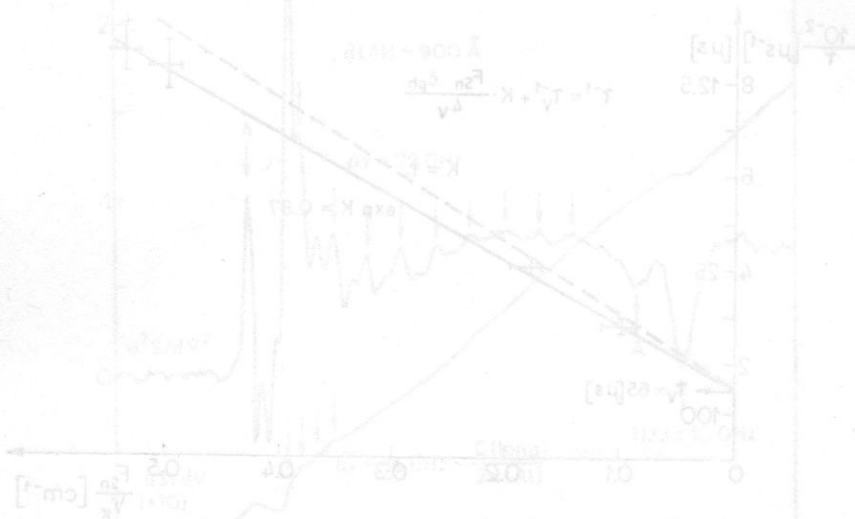


Fig. 17. The relation between the real and imaginary parts of the complex propagation constant K . The real part is shown in solid lines and the imaginary part in dashed lines. The experimental data points are shown as open circles. The solid line is a fit to the experimental data. The dashed line is a fit to the experimental data. The solid line is a fit to the experimental data. The dashed line is a fit to the experimental data.